Original Article

MOLECULAR METABOLISM

# Adipose TBX1 regulates β-adrenergic sensitivity in subcutaneous adipose tissue and thermogenic capacity in vivo

**Kathleen R. Markan [1,2,*], Lauren K. Boland [2,5], Abdul Qaadir King-McAlpin [1,2], Kristin E. Claflin [1,2,3], Michael P. Leaman [1,2], Morgan K. Kemerling [1,2], Madison M. Stonewall [1,2], Brad A. Amendt [4], James A. Ankrum [2,5], Matthew J. Potthoff [1,2,3,6]**

## ABSTRACT

**Objective:** T-box 1 (TBX1) has been identified as a genetic marker of beige adipose tissue. TBX1 is a mesodermal development transcription factor essential for tissue patterning and cell fate determination. However, whether it plays a role in the process of adipose beiging or how it functions in adipose tissue has not been reported. Here, we examined the function of TBX1 in adipose tissue as well as adipose-derived stem cells from mice and humans.

**Methods:** Adipose-specific TBX1 transgenic (TBX1 AdipoTG) and adipose-specific TBX1 knockout (TBX1 AdipoKO) mice were generated to explore the function of TBX1 in the process of adipose beiging, metabolism and energy homeostasis in vivo. In vitro, we utilized a siRNA mediated approach to determine the function of TBX1 during adipogenesis in mouse and human stem cells.

**Results:** Adipose-specific overexpression of TBX1 was not sufficient to fully induce beiging and prevent diet-induced obesity. However, adipose TBX1 expression was necessary to defend body temperature during cold through regulation of UCP1 and for maintaining β3-adrenergic sensitivity and glucose homeostasis in vivo. Loss of adipose TBX1 expression enhanced basal lipolysis and reduced the size of subcutaneous iWAT adipocytes. Reduction of TBX1 expression via siRNA significantly impaired adipogenesis of mouse stromal vascular cells but significantly enhanced adipogenesis in human adipose derived stem cells.

**Conclusions:** Adipose expression of TBX1 is necessary, but not sufficient, to defend body temperature during cold via proper UCP1 expression. Adipose TBX1 expression was also required for proper insulin signaling in subcutaneous adipose as well as for maintaining β-adrenergic sensitivity, but overexpression of TBX1 was not sufficient to induce adipocyte beiging or to prevent diet-induced obesity. TBX1 expression is enriched in adipose stem cells in which it has contrasting effects on adipogenesis in mouse versus human cells. Collectively, these data demonstrate the importance of adipose TBX1 in the regulation of beige adipocyte function, energy homeostasis, and adipocyte development.



**Keywords** Tbx1; Beige; Brite; Adipose; Subcutaneous; Thermogenesis

## 1. INTRODUCTION

Adipose tissue is a dynamic endocrine organ consisting of a heterogenous cell population including mature adipocytes, pre-adipocytes, immune cells, endothelial cells, progenitor cells and stem cells [1]. In a healthy state, adipose tissue responds to nutritional status and various hormonal inputs to coordinate energy utilization, storage and mobilization [2]. There are multiple types of adipocytes including white, beige/brite, and brown adipocytes. Classical white adipocytes are unilocular lipid laden cells that store or mobilize energy into circulation in response to insulin versus catecholaminergic signaling [1]. However, the accrual of excess white adipose is a hallmark of obesity and precipitates many other metabolic disorders, in part because of an excess nutrient load [3]. In contrast to white adipocytes, brown adipocytes are multilocular cells that dissipate energy as heat through the process of adaptive thermogenesis [4]. This ability of brown adipocytes to generate heat is mediated by the expression of a specialized mitochondrial uncoupling protein-1 (UCP1), which is an essential means for rodents and small mammals to maintain thermoregulation [4]. Beige adipocytes are unique in that they share similarities with both white and brown adipocytes. Under normal conditions, beige adipocytes appear phenotypically similar to white adipocytes, but can be induced into multilocular, mitochondrial dense adipocytes that express abundant levels of UCP1 [5]. When induced through β-

[1]Department of Neuroscience and Pharmacology, Iowa City, IA, 52242, USA [2]Fraternal Order of Eagles Diabetes Research Center, Iowa City, IA, 52242, USA [3]Iowa Neurosciences Institute, Iowa City, IA, 52242, USA [4]Department of Anatomy and Cell Biology and the Craniofacial Anomalies Research Center, Iowa City, IA, 52242, USA [5]Roy J. Carver Department of Biomedical Engineering, University of Iowa Carver College of Medicine, Iowa City, IA, 52242, USA [6]Department of Veterans Affairs Medical Center, Iowa City, IA, 52242, USA

*, Corresponding author. University of Iowa Carver College of Medicine, 169 Newton Road, 3459 PBDB, Iowa City, IA, 52242, USA. Fax: 319 335 8930. E-mail: krmarkan@gmail.com (K.R. Markan).

Received December 20, 2019 • Revision received February 7, 2020 • Accepted February 11, 2020 • Available online 18 February 2020

https://doi.org/10.1016/j.molmet.2020.02.008

 

adrenergic signaling, beige adipocytes emerge within white adipose, a process referred to as adipose 'beiging' [6]. UCP1 expressing adipocytes are uniquely endowed with the ability to clear copious amounts of plasma glucose and lipid concomitant to β-adrenergic stimulated lipolysis [7]. Additionally, genetic and pharmacological models of enhanced adipose beiging are protected from diet-induced obesity and its deleterious effects on metabolism [6,8,9]. Therefore understanding the mechanism governing the development and metabolic properties of beige adipose is therapeutically imperative [10—12].

Beige adipocytes develop either through de novo adipogenesis or through the 'trans-differentiation' of mature white adipocytes into active UCP1 expressing beige adipocytes [13—17] or some combination of the two. While cell surface markers of mature beige adipocytes and beige adipocyte progenitor cells have been identified [18,19], few bona fide genetic markers of beige adipocytes have been validated [20]. Of these genes, the transcription factor T-box 1 (TBX1) has been utilized as a beige adipose marker in both mice and humans [14,20—22]. Although TBX1 mRNA has been reported to be expressed at a greater level in beige adipose tissue in vivo and ex vivo [14,20—22], its use as a beige adipocyte marker in vitro may be less specific as its expression is lost over time, suggesting yet unknown external regulatory factors [20]. TBX1 is a mesodermal development gene belonging to the T-box family, which are key regulators of development throughout metazoans [23]. TBX1 is essential during embryogenesis for tissue formation, cell fate determination and proliferation (reviewed in [24]). Individuals diagnosed with 22q11.2 deletion syndrome have a chromosomal microdeletion spanning the TBX1 gene, making it a candidate gene for deficits including but not limited to immunodeficiency, hypoparathyroidism and congenital heart disease [25]. Many T-box family proteins bind to non-identical palindromic consensus DNA sequences termed T-boxes in order to regulate transcription [23] and two slightly permutated consensus T-box binding sequences have been identified for TBX1 [26,27]. However, more recent studies indicate that TBX1 is neither a strong transcriptional repressor nor activator [24] but rather, exerts effects on transcription through off-DNA protein-protein interactions including SMAD1, histone methyltransferases and components of the chromatin remodeling complex [27—29].

Despite these studies, no investigations concerning the function of TBX1 specifically in adipose tissue have been reported. Here, we generated novel adipose-specific gain- and loss-of-function mouse models to test the role of TBX1 in adipose tissue beiging, metabolism and energy homeostasis. Our studies reveal that TBX1 expression in mature adipose is required for full UCP1 activity and the maintenance of body temperature during cold, but overexpression of TBX1 is not sufficient to drive beiging and prevent the development of diet-induced obesity. Furthermore, adipose TBX1 is required for proper subcutaneous adipose insulin signaling and β-adrenergic sensitivity and glucose homeostasis in vivo. Collectively, these data demonstrate that TBX1 is a novel regulator of adipose tissue function and whole-body metabolism.

## 2. MATERIALS AND METHODS

### 2.1. Animals

Adiponectin-Cre transgenic mice, TBX1 COET mice and TBX1fl/fl mice have all been previously reported [30—32]. TBX1fl/fl mice possess a loxP flanked exon 5 such that upon Cre-recombinase mediated recombination this exon is excised [32]. Excision of exon 5, which encodes the T-box domain, and splicing between exons 4 and 6, causes a frame shift resulting in a premature stop codon and subsequent loss of function [32]. Adipocyte-specific TBX1 transgenic mice were generated by crossing Adiponectin-Cre transgenic mice with TBX1 COET mice while adipocyte specific TBX1 knockout mice were generated by crossing adiponectin-cre transgenic mice with TBX1fl/fl mice. All mice used in these studies were male on a C57Bl6/J background maintained on standard chow (2920X; Envigo) or fed a 60% high fat diet (HFD; Research Diets, D12492i) for 7 weeks. Mice were at least 6-weeks-old when placed on HFD. Mice were maintained on a 12:12 h light: dark cycle and all procedures were approved by the University of Iowa IACUC. For all experiments, littermate control mice were used.

### 2.2. Thermoneutrality and cold exposure studies

For studies at thermoneutrality or involving cold exposure, mice were housed in an environmental chamber (Powers Scientific, Inc.) set to either 30 °C (TN; thermoneutrality) or 4 °C. Rectal temperatures were measured using a dual channel Traceable Expanded Range Probe (Fisher Scientific).

### 2.3. Mouse adipocyte studies

Stromal vascular cells were isolated from 4-6-day old wild type neonates and differentiated as previously described [33]. Briefly, cells were in DMEM supplemented with 10% FBS and 5% pen-strep, non-essential amino acids, Glutamax, 1 M HEPES, and 0.1 mM β-mercaptoethanol until confluent. Forty-eight hours post-confluency cells were placed into new media containing DMEM supplemented with 10% FBS, 5% pen-strep, 1 μM dexamethasone, 0.5 mM IBMX, and 5 μg/mL insulin for 48 h. Adipocytes were then cultured in supplemented DMEM containing 5 μg/mL of insulin until the experiment. For experiments, adipocytes were placed into serum-free media containing either vehicle or 1 μM isoproterenol for 16 h and then collected for RNA isolation.

Collagenase isolation of primary adipocytes was performed in the following manner. Mice were euthanized and iWAT quickly dissected out and placed into 37 °C Hanks buffer containing 3% BSA and 2 mg/mL of collagenase II (Worthington). Tissue was finely minced with surgical scissors and then incubated at 37 °C with gentle shaking for 45 min. The tissue was then poured through a nylon mesh and gently centrifuged 500×*g* for 2 min in order to allow primary adipocytes to float to top of surface. Primary adipocytes were then gently washed 3 times with collagenase-free Hanks buffer.

### 2.4. Gene and protein expression studies

RNA isolation and gene expression analysis was performed as described [34]. QPCR primer sequences follow: mouse Tbp1 forward 5′-CACAGGAGCCAAGAGTGAAGA-3′ reverse 5′- AGAACTTAGCTGGGAAGCCC; mouse Tbx1 used for expression profiling forward 5′-GGCAGGCAGACGAATGTTC-3′ and reverse 5′- TTGTCATCTACGGGCACAAAG-3′; mouse Tbx1 used for confirming genetic deletion forward 5′-AGAATCACCGGATCACGCAG-3′ and reverse 5′-GTCCTCCGGGTCGCAATC-3′; mouse Cebpa forward 5′- TGGCCTGGAGACGCAATGA-3′ and reverse 5′- CGCAGAGATTGTGCGTCTTT-3′; mouse Pparg forward 5′- GCATGGTGCCTTCGCTGA-3′ and reverse 5′-TGGCATCTCTGTGTCAACCATG-3′; mouse Prdm16 forward 5′- TGACCATACCCGGAGGCATA-3′ and reverse 5′- CTGACGAGGGTCCTGTGATG-3′; mouse Ucp1 forward 5′- CGGGCATTCAGAGGCAAATC-3′ and reverse 5′- CCGAGAGAGGCAGGTGTTTC-3′; mouse Ppargc1a forward 5′- AGACAAATGTGCTTCCAAAAAGAA-3′ and reverse 5′- GAAGAGATAAAGTTGTTGGTTTGGC- 3′; mouse Cd137 forward 5′- CGTGCAGAACTCCTGTGATAAC-3′ and reverse 5′-GTCCACCTATGCTGGAGAAGG-3′; mouse Tmem26 forward 5′-

 

ACCCTGTCATCCCACAGAG-3′ and reverse 5′- TGTTTGGTGGAGTCC-TAAGGTC-3′; mouse Adipoq forward 5′- TGTCCCCATGAGTACCAGACT-3′ and reverse 5′- TCCTGAGCCCTTTTGGTGTC-3′; mouse Fabp4 forward 5′-AGTGAAAACTTCGATGATTACATGAA-3′ and reverse 5′-GCCTGCCACTTTCCTTGTG-3′.

Human TBP1 forward 5′- CAC GAA CCA CGG CAC TGA TT-3′ and reverse 5′- TTT TCT TGC CAG TCT GGA C-3′; human TBX1 forward 5′-ACGACAACGGCCACATTATTC-3′ and reverse 5′- CCTCGGCA-TATTTCTCGCTATCT-3′; human CEBPA forward 5′-TATAGGCTGGGCTTCCCCTT- 3′ and reverse 5′- AGCTTTCTGGTGT-GACTCGG-3′; human PPARG forward 5′- ACCCAGAAAGCGATTCCTTCA-3′ and reverse 5′- TGTGTCAACCATGGTCATTTCTTG-3′; human ADIPOQ forward 5′- GGAGATCCAGGTCTTATTGGTCC-3′ and reverse 5′-TTTCCTGCCTTGGATTCCCG-3′; human FABP4 forward 5′-TGGGCCAGGAATTTGACGAA-3′ and reverse 5′- CACATGTACCAGGA-CACCCC-3′; human PLN forward 5′- CCCAGGAGTGACAGGAATTGTT-3′ and reverse 5′- ATCCTCGCTCCTCAAGTCCG-3′.

For protein analysis, tissues were homogenized on ice and lysate prepared as previously described [34]. Bradford assay was performed to determine protein concentration and then equal amounts of protein were resolved by SDS-PAGE, transferred to PVDF membrane and then probed with specific antibodies: anti-UCP1 (Abcam #10983) and β-actin (Sigma #A5316), phoshpo-ERK1/2 (Cell Signaling Technology #9101), total ERK1/2 (Cell Signaling Technology #9102), phospho-mTOR (Cell Signaling Technology #5536), total mTOR (Cell Signaling Technology #2983), phospho-Akt (Cell Signaling #9271), and total Akt (Cell Signaling Technology #9272).

### 2.5. Assessment of mitochondrial respiration

Mitochondria were isolated based on [35] with modifications for adipose tissue. Briefly, iWAT was immediately collected following euthanasia and placed into ice cold mito isolation buffer containing 70 mM sucrose, 210 mM mannitol, 5 mM HEPES pH 7.4, and 1 mM EGTA. Tissue was minced finely with surgical scissors and then homogenized using a glass grinder and Teflon pestle rotating at 275 rpm. Homogenate was centrifuged at 700×*g* for 10 min at 4 °C. Supernatant was collected and centrifuged at 8500×*g* for 10 min at 4 °C to pellet mitochondria. The mitochondrial pellet was resuspended in fresh mito isolation buffer and mitochondrial protein concentration determined via Bradford Assay. Mitochondria were plated at 2 μg/well in mitochondria respiration buffer containing 70 mM sucrose, 210 mM mannitol, 10 mM K2PO4, 5 mM MgCl2, 5 mM HEPES pH 7.4, 1 mM EGTA, 10 mM malate, 5 mM pyruvate and 0.20% BSA free-fatty acid free. Basal oxygen consumption rate was then determined via Seahorse Bioflux Analyzer (University of Iowa ESR Core).

### 2.6. Glucose and insulin tolerance tests

For glucose tolerance tests, mice were fasted for 6 h and time 0 blood was collected via tail bleed followed by an intraperitoneal (i.p.) injection of glucose at 2 g glucose/kg total body weight in lean chow fed animals and 1.3 g glucose/kg total body weight for high fat fed animals. For insulin tolerance tests, mice were fasted for 4 h and time 0 blood was collected via tail bleed followed by an i.p. injection of insulin at 0.75 U/kg total body weight. Tail blood was then collected over the course of 120 min, processed and analyzed as described previously [34]. Glucose and insulin tolerance tests were performed either at room temperature (∼22 °C) or thermoneutrality (∼30 °C) as indicated. To assess glucose tolerance in response to β3-adrenergic receptor activation, a cohort of wild type mice were injected the day of the GTT with vehicle or CL316,243 (0.25 mg/kg body weight) 6 h prior to time 0 of the GTT. Likewise, a cohort of TBX1 AdipoTG mice were injected on the day of the GTT with vehicle or CL316,243 (0.25 mg/kg body weight) 6 h prior to time 0 of the GTT. To stimulate adipose beiging independent of cold exposure, wild type mice were injected with either vehicle or CL316,243 (1 mg/kg body weight) once daily for 3 days [36] with the final injection occurring 6 h prior to time 0 of the GTT. The same design was repeated with a cohort of TBX1 AdipoKO mice.

### 2.7. Insulin and β-adrenergic signaling assays

To assess insulin signaling in adipose tissue, TBX1 AdipoKO and littermate control mice were fasted for 4 h and then euthanized. The iWAT depots were pooled per genotype in KRB buffer containing HEPES pH 7.4 supplemented with 5 mM glucose. Samples were then finely minced ∼200X with surgical scissors and then equal amounts of minced tissue were plated into wells of tissue culture plate containing the described buffer with vehicle, 1 nM, 5 nM, 10 nM or 100 nM of insulin and then incubated at 37 °C for 10 min with gentle shaking. Plates were placed on ice and tissue immediately collected for protein isolation. To assess β3-receptor mediated adrenergic signaling, iWAT from TBX1 AdipoKO and littermate control mice was prepared as described above and incubated in buffer containing vehicle, 0.01 μM, 0.1 μM, 1 μM or 10 μM CL316,243 and incubated at 37 °C for 10 min with gentle shaking. Plates were placed on ice and tissue was immediately collected for protein isolation.

### 2.8. Histology, immunohistochemistry, and adipocyte size analysis

The iWAT of male wild type and TBX1 AdipoKO littermates, 10—12 weeks of age, was collected into 4% paraformaldehyde and incubated for 48 h at 4 °C with gentle shaking. Tissues were processed, and H&E staining was performed via the Pathology Core (University of Iowa). For immunohistochemistry, slides were incubated in UCP1 (Abcam #10983 at 1:500) and perilipin (Abcam #61682 at 1:100) antibodies overnight at 4 °C followed by Alexa Fluor anti-rabbit 488 and 568 secondary antibodies. Slide images were captured using an Olympus IX83 microscope and adipocyte size analyzed using ImageJ platform (National Institutes of Health).

### 2.9. Human MSC isolation and characterization

Mesenchymal stromal cells from three human donors and tissue sources (bone marrow, adipose tissue, and umbilical cord) were isolated and expanded for baseline TBX1 interrogation. Bone marrow donor 00082 was purchased from and confirmed to meet ISCT MSC Minimal Criteria [37] by RoosterBio followed by outgrowth and cryobanking under standard protocols, as previously described [38]. Umbilical cord mesenchymal stromal cell (ucMSC) donor 4600 was isolated via tissue explant method from Wharton's Jelly using standard FBS-supplemented media or human platelet lysate supplemented media. Following isolation, ucMSCs were outgrown, cryobanked, and MSC identification was confirmed by immunophenotyping and trilineage differentiation under their respective media formulations, as previously described [39]. Adipose tissue MSCs (adMSCs) were isolated from human stromal vascular fractions after enzymatic degradation of subcutaneous adipose tissue, as previously described [40]. Immunophenotyping of adMSCs was performed using the following antibodies: FITC-CD105 (BD Biosciences, Cat #561443), PE-CD90 (Invitrogen, Cat #A15794), and PE.Cy7-CD73 (BD Biosciences, Cat #561258) with isotype controls (FITC Mouse IgG1k, PE.Cy7 Mouse IgG1k, and PE-CD90 Mouse IgG1k). Absence of CD45, CD34, CD11b, CD19, and HLA-DR was confirmed using the PE hMSC Negative Cocktail (BD Biosciences, Cat #562530), as per the manufacturer's instructions. Adipogenic and osteogenic differentiation was performed over a 15-day period (Biological Industries, Cat #05-330-1 B-KT and

 

Cat #05-440-1 B) followed by staining with AdipoRed and Alizarin Red, respectively, as previously described [39].

### 2.10. Human adipose derived MSC culture and differentiation

After initial isolation and preliminary expansion, adipose derived MSCs were cryopreserved at 1 million cells/mL using CryoStor CS5 Freeze Media and stored in liquid nitrogen until experimental use. For cell outgrowth, adipose derived MSCs were plated at a density of ~3000 cells/cm2 and grown in standard MSC growth media (MEM-alpha without nucleosides supplemented with 15% FBS, 1% pen-strep, and 1% L-glutamine) until reaching 70–80% confluence. All experiments were performed using adipose derived MSCs at passage 3–5, with all frozen stocks initially preserved at P2. For adipogenic differentiation and gene expression studies, adipose derived MSCs were switched into an adipogenic differentiation cocktail consisting of high-glucose DMEM supplemented with 10% FBS, 1% pen-strep, 1 μM dexamethasone, 0.5 mM IBMX, and 5 μg/mL insulin for 7 days, with fresh media exchange at day 3 post-differentiation.

### 2.11. TBX1 siRNA adipogenesis studies

Isolated mouse and human cells were reseeded and transduced the following day near ~80% confluence with a negative control scrambled siRNA (Thermo; #4390843) or siRNA targeting mouse or human TBX1 respectively. For mouse cell studies, Thermo #4390771; ID s74769 targeting exon 5 at base pair 748 was used. For human cell studies, Thermo #4392420; ID s13801 targeting exon 6 at base pair 856 was used. To assess transfection efficiency, mouse and human adipose derived cells were transfected with a negative control scrambled siRNA or TYE53-linked siRNA (IDT, Inc.) and transfection efficiency assessed via Flow Cytometry 24- and 48-hours post-transfection. Cells were transfected using Lipofectamine RNAiMAX (Thermo) as per the manufacturer's instructions. Post-transduction, cells were incubated for 48 h in growth media before beginning species-specific adipogenesis protocol.

### 2.12. Plasma analysis

Plasma metabolites were analyzed using colorimetric kits per the manufacturer's instructions as previously described [34].

### 2.13. Data analysis

Data were analyzed using Excel or GraphPad Prism 7 and statistical differences between groups were determined via the Student's t-test or two-way ANOVA utilizing Sidak's correction for multiple comparisons.

## 3. RESULTS

### 3.1. Generation of adipose-specific TBX1 transgenic and knockout mice

To begin to investigate the function of TBX1 in adipose, we profiled Tbx1 mRNA expression in adipose depots of wild-type mice. Tbx1 mRNA was most highly expressed in subcutaneous inguinal white adipose tissue (iWAT), a depot highly susceptible to beiging [42] (Figure 1A). Further profiling revealed comparable expression levels of Tbx1 in mature adipocytes and stromal vascular cells isolated from iWAT of male C57Bl6 mice (Figure 1B). Although the utility of TBX1 as a genetic marker of beiging in vivo versus in vitro has been debated [14,20–22], nothing has been reported regarding its function in adipose tissue. Therefore we generated adipose-specific TBX1 transgenic (TBX1 AdipoTG) and knockout (TBX1 AdipoKO) mice to test if TBX1 was sufficient and necessary to induce the beiging of adipose tissue. TBX1 AdipoTG mice were generated by crossing adiponectin-Cre transgenic mice with TBX1 COET mice, which contain a chicken beta-actin promoter, a neomycin cassette flanked by LoxP sites followed by mouse TBX1 cDNA [31]. Tbx1 and Ucp1 mRNAs were significantly increased in the iWAT of TBX1 AdipoTG mice (Figure 1C–D) and UCP1 protein remained increased in the iWAT of TBX1 AdipoTG mice housed at thermoneutrality (30 °C; Figure 1E). However, no differences were detected in beige cell formation between genotypes as determined via UCP1 immunofluorescence (Supplementary Figure. 1G), indicating that TBX1 likely regulates UCP1 expression in previously existing beige cells. Although Tbx1 mRNA was also increased in the BAT and eWAT of these mice, no changes were detected in Ucp1 expression in these tissues (Supplementary Figures. 1A–D), indicating that TBX1 likely functions in an iWAT specific manner. Finally, Tbx1 mRNA was unchanged in the livers of TBX1 AdipoTG mice confirming tissue-specific specificity of transgene expression (Supplementary Figures. 1E–F).

To generate TBX1 AdipoKO mice, TBX1fl/fl mice [32] were crossed with adiponectin-Cre transgenic mice. Using primers specific for the floxed exon 5 of TBX1, Tbx1 mRNA was significantly decreased in whole iWAT (Figure 1F) and in primary adipocytes isolated via collagenase from the iWAT of TBX1 AdipoKO mice (Supplementary Figure. 1H); however, no change in Ucp1 mRNA was detected (Figure 1G). Furthermore, there was no difference in the number of UCP1 positive adipocytes determined via immunofluorescent staining in the iWAT of wild type versus TBX1 AdipoKO mice housed at room temperature (Supplementary Figure 1P). Ucp1 mRNA levels were also unchanged in BAT of TBX1 AdipoKO mice despite increased Tbx1 mRNA expression (Supplementary Figs. 1I–J), and no changes in eWAT Tbx1 or Ucp1 mRNA were detected (Supplementary Figure. 1K-L). No alterations in gene expression were detected in livers of TBX1 AdipoKO mice, again demonstrating specificity (Supplementary Figure 1M–N).

### 3.2. Adipose TBX1 expression is necessary to maintain body temperature during cold exposure

Beige adipocytes are induced by increased sympathetic nerve activation and β-adrenergic signaling in response to sub-thermoneutral temperatures [43]. To determine if loss of TBX1 in adipocytes affects adipocyte metabolism in response to β-adrenergic signaling, we isolated stromal vascular cells from the iWAT of neonatal wild type and TBX1 AdipoKO mice, which were cultured and differentiated to similar degrees into adipocytes in vitro (Supplementary Figure 1O). Differentiated adipocytes were then treated with vehicle or the β-adrenergic agonist isoproterenol. While *Ucp1* mRNA was robustly induced in wild type adipocytes treated with isoproterenol, *Ucp1* levels were significantly blunted in isoproterenol treated TBX1 AdipoKO adipocytes relative to wild type adipocytes (Figure 1H). Additionally, respiration of mitochondria isolated from the iWAT of cold exposed TBX1 AdipoKO mice was also significantly decreased relative to cold exposed controls (Figure 1I), most likely due to a blunted expression of UCP1 protein in iWAT following cold exposure (Supplementary Figure 1Q). Collectively, this data links impaired UCP1 expression in the subcutaneous adipose of TBX1 AdipoKO mice in vivo with impaired subcutaneous derived mitochondrial respiration ex vivo.

Based on the increased iWAT UCP1 expression in TBX1 AdipoTG mice, we next tested whether TBX1 may be sufficient to increase beiging of subcutaneous white adipose in vivo. TBX1 AdipoTG mice were acclimated at thermoneutrality 30 °C for 4 days and then housed at 4 °C for 5 h. TBX1 AdipoTG mice had a greater decrease in body temperature relative to littermate controls following 1 h at 4 °C but quickly recovered to control levels within 2 h of cold onset (Figure 1J, left). The rate of body temperature change in TBX1 AdipoTG mice was

 

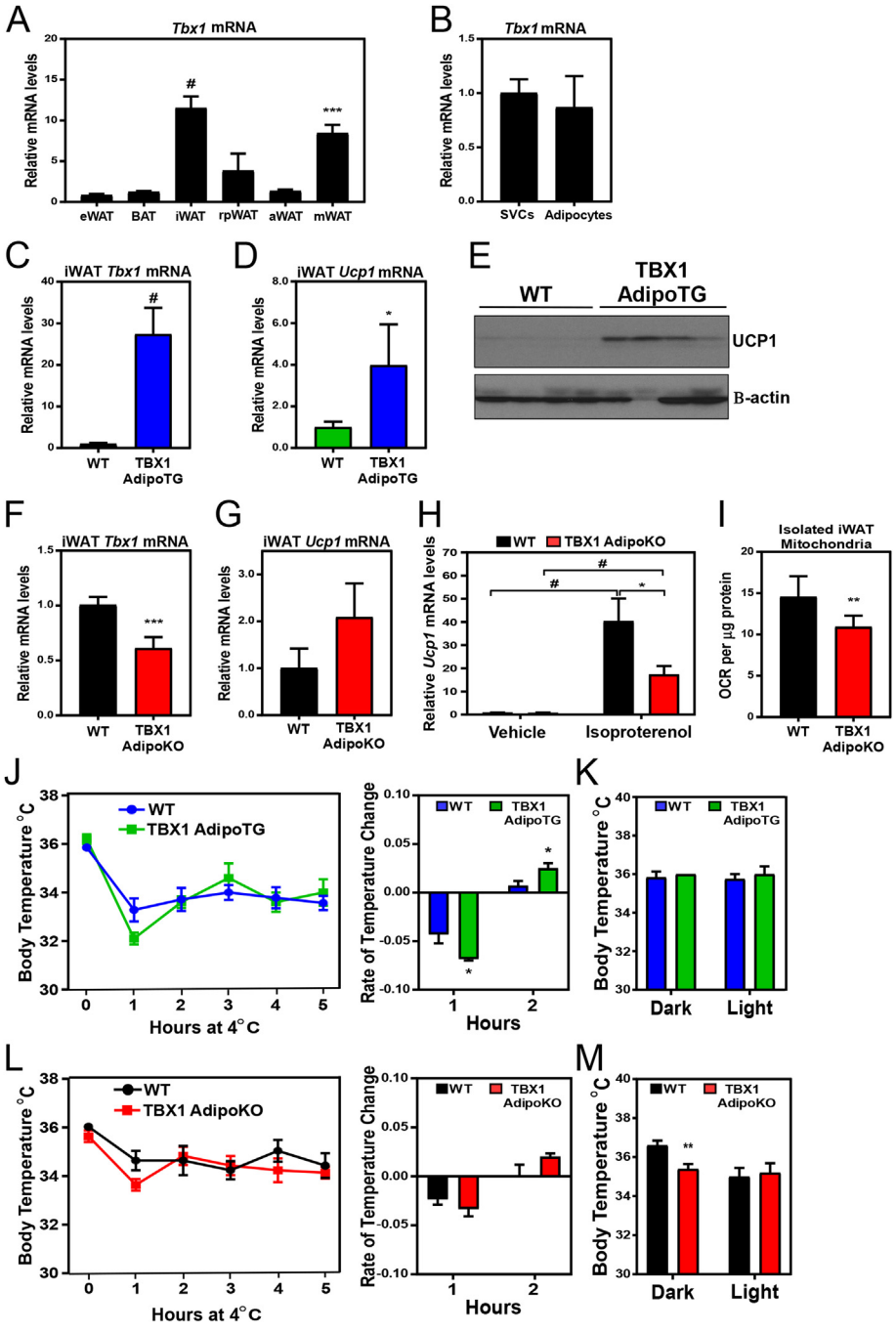


**Figure 1: Adipose TBX1 is necessary to maintain body temperature during cold exposure**. (A) Expression levels of *Tbx1* mRNA in adipose depots of 10-week old C57Bl6 male mice (n = 3). (B) *Tbx1* mRNA expression levels in collagenase isolated stromal vascular cells versus mature adipocytes in iWAT pooled from 8-week old C57Bl6 male mice (n = 3). (C–D) *Tbx1* and *Ucp1* mRNA levels in the iWAT of wild type (WT) and TBX1 AdipoTG mice (n = 9–11/group). (E) UCP1 protein content in the iWAT of wild type (WT) and TBX1 AdipoTG mice at 30 °C (n = 4/group). (F–G) *Tbx1* and *Ucp1* mRNA levels in whole iWAT of wild type (WT) and TBX1 AdipoKO mice (n = 5–9/group). (H) *Ucp1* mRNA levels of in vitro differentiated adipocytes isolated from wild type (WT) and TBX1 AdipoKO mice and then treated with vehicle or isoproterenol (n = 3; performed in technical triplicates; cells pooled from 5 to 8 pups per experiment). (I) Basal oxygen consumption rates of mitochondria isolated from the iWAT of wild type (WT) and TBX1 AdipoKO mice housed at 4 °C (n = 4–5/group). (J, left) Body temperature of wild type (WT) and TBX1 AdipoTG mice at thermoneutrality (time 0) and through 5 h at 4 °C and (J, right) the rate of change in body temperature over the first 2 h at 4 °C shown in left (n = 5–7/group). (K) Body temperature of wild type (WT) and TBX1 AdipoTG mice during the dark phase and the light phase following 72 h at 4 °C (n = 4–6/group). (L, left) Body temperature of wild type (WT) and TBX1 AdipoKO mice at thermoneutrality (time 0) and through 5 h at 4 °C and (L, right) the rate of change in body temperature over the first 2 h at 4 °C shown in left (n = 5/group). (M) Body temperature of wild type (WT) and TBX1 AdipoKO mice during the dark phase and the light phase following 72 h at 4 °C (n = 5/group). Values are mean ± SEM; *, $p \leq 0.05$; **, $p \leq 0.001$; ***, $p \leq 0.005$; #, $p \leq 0.001$.

 

significantly accelerated relative to control mice in the first and second hours of cold exposure (Figure 1J, right). Next, TBX1 AdipoTG mice were subjected to a chronic cold challenge. Following acclimation at 30 °C, TBX1 AdipoTG and littermate controls were housed at 4 °C for 3 days. No differences were detected between genotypes in body temperature during the dark or light phases following 3 days of cold (Figure 1K) indicating that although overexpression of adipose TBX1 increases iWAT UCP1 expression, it is not sufficient to prevent a decrease in body temperature in response to cold.

Since TBX1 AdipoKO mice displayed reduced UCP1 expression and mitochondrial respiration in iWAT, after cold exposure, we next repeated the acute and chronic cold challenges using these mice. No significant changes were observed in absolute body temperature or the rate of body temperature change in TBX1 AdipoKO mice during an acute 5-hour cold challenge (Figure 1L, left & right). However, following 3 days at 4 °C, TBX1 AdipoKO mice displayed significantly lower body temperatures during the final dark phase relative to control mice (Figure 1M). Collectively, these data indicate that TBX1 functions in existing beige cells to regulate UCP1 expression and body temperature during cold exposure.

### 3.3. Adipose TBX1 function is necessary for maintaining in vivo glucose homeostasis

Since genetic and pharmacological models of adipose beiging enhance metabolism and can prevent diet induced obesity [6,8,9], we tested the impact of adipose TBX1 overexpression and deletion on energy homeostasis in chow fed and high fat fed mice. TBX1 AdipoKO mice fed standard chow had similar body weights (Figure 2A) and fed plasma metabolite levels as wild type littermates (Supplementary Table 1). However, in the fasted state, TBX1 AdipoKO mice had significantly higher plasma glucose levels compared to fasted control mice (Supplementary Table 1). However, fasted TBX1 AdipoKO plasma insulin levels were not statistically different from controls (Supplementary Table 1; p-value = 0.08) To investigate this further, insulin tolerance tests were performed. Chow fed TBX1 AdipoKO mice and wild type littermates displayed similar plasma glucose levels within the first 60 min of insulin injection (Figure 2B). However, during the two lattermost time points of the ITT (time 90 and 120 min), TBX1 AdipoKO mice displayed significantly elevated plasma glucose levels versus controls (Figure 2B); suggesting a potentially enhanced counterregulatory response to decreased plasma glucose during the preceding time points [44,45]. Since UCP1 positive adipocytes are activated by β-adrenergic signaling, as occurs during cold exposure, and can clear significant levels of plasma glucose [7], we next performed glucose tolerance tests using chow fed wild type and TBX1 AdipoKO mice following 3 days of treatment with vehicle or the $\beta_3$-adrenergic agonist CL316,243 in order to mimic cold exposure. Both genotypes displayed enhanced clearance of plasma glucose following treatment with CL316,243 versus vehicle (Figure 2C–E) indicating intact β-adrenergic responsiveness in vivo. In contrast to studies with chow fed TBX1 AdipoKO mice, we did not observe any alterations in body weight, glucose homeostasis or plasma metabolite levels of chow fed TBX1 AdipoTG mice housed at thermoneutrality (Supplementary Figures. 2A–C and Supplementary Table 2), indicating that overexpression of TBX1 in adipose does not alter energy homeostasis.

Despite the lack of metabolic phenotype in chow fed TBX1 AdipoTG mice and because of the increased UCP1 content observed in TBX1 AdipoTG mice, we next sought to determine if adipose specific overexpression of TBX1 was sufficient to prevent the development of diet-induced obesity and its deleterious metabolic effects. Surprisingly, TBX1 AdipoTG mice housed at thermoneutrality were not protected against weight gain on a high fat diet (Supplementary Figure. 2D) and no differences were observed versus high fat fed wild type mice in glucose homeostasis in response to vehicle or treatment with CL316,243 (Supplementary Figures. 2E–F). Similarly, high fat fed TBX1 AdipoKO mice gained weight at the same rate as wild type mice and displayed comparable insulin sensitivity during an ITT (Figure 2F–G). High fat fed wild type mice treated with CL316,243 for 3 days were significantly more glucose tolerant compared to littermate controls treated with vehicle (Figure 2H,J). Finally, unlike in the chow fed condition, high fat fed TBX1 AdipoKO mice failed to increase clearance of plasma glucose following CL316,243 treatment (Figure 2I–J).

### 3.4. Loss of adipose TBX1 impairs insulin signaling and enhances basal lipolysis in subcutaneous adipose tissue

In order to determine if loss of adipose TBX1 in subcutaneous adipose contributes to the metabolic phenotype of TBX1 AdipoKO mice observed in vivo, we assessed insulin signaling using iWAT explants of lean WT and TBX1 AdipoKO mice. Levels of Akt phosphorylation were decreased in TBX1 AdipoKO iWAT compared to wild type iWAT treated in vitro with increasing doses of insulin (Figure 3A). Additionally, the release of non-esterified fatty acids (NEFAs) was significantly increased in TBX1 AdipoKO iWAT explants relative to control explants cultured in vitro under basal conditions and in response isoproterenol treatment although not significantly (Figure 3B). Histological analysis revealed that adipocytes from the iWAT of TBX1 AdipoKO mice were on average smaller and more numerous than wild type mice in both the chow and the high fat diet conditions (Figure 3C–J) indicating the loss of adipose TBX1 results in altered insulin signaling and hyperplasia of hypotrophic adipocytes independent of nutritional context.

### 3.5. TBX1 differentially regulates adipogenesis in adipose derived mouse versus human stem cells

In our initial profiling of *Tbx1* expression across mouse adipose depots, we found that *Tbx1* mRNA was highly expressed in stromal vascular cells isolated from iWAT of wild type mice (Figure 1B), suggesting that TBX1 could function in this population of cells potentially to regulate adipocyte development. To test this, we used an siRNA mediated approach. A siRNA specific for mouse *Tbx1* was selected as previously described [27], and both siRNA knockdown of *Tbx1* expression and transfection efficiency using TYE 563 DsiRNA (IDT, Inc.) were verified using stromal vascular cells isolated from wild type neonatal mice (Supplementary Figures. 3A–B). To test the role of TBX1 in adipocyte development, wild type neonatal mouse stromal vascular cells were isolated, cultured in vitro, transduced with either a negative control scrambled siRNA or a siRNA targeting *Tbx*1, and then differentiated into adipocytes per standard protocol [33]. As seen in Figure 4A, *Tbx1* expression was significantly decreased in cells transfected with the *Tbx1* siRNA, resulting in significantly decreased expression of key adipogenic genes including *Cebpα* and *Pparg* indicating that *Tbx1* expression is required for full differentiation of mouse stromal vascular cells into adipocytes. Notably, TBX1 has been reported to play a role in stem cell renewal in other tissue types [46–48] and, although TBX1 is detectable in human adipose [21,22], nothing has been reported regarding its potential role in human adipogenesis. To address this, we profiled *TBX1* expression in mesenchymal stem cells (MSCs) isolated from various human tissue sources and found *TBX1* to be significantly enriched in human adipose derived mesenchymal stem cells versus those isolated from umbilical cord or bone marrow (Figure 4B). We confirmed that the TBX1 expressing human adipose

 

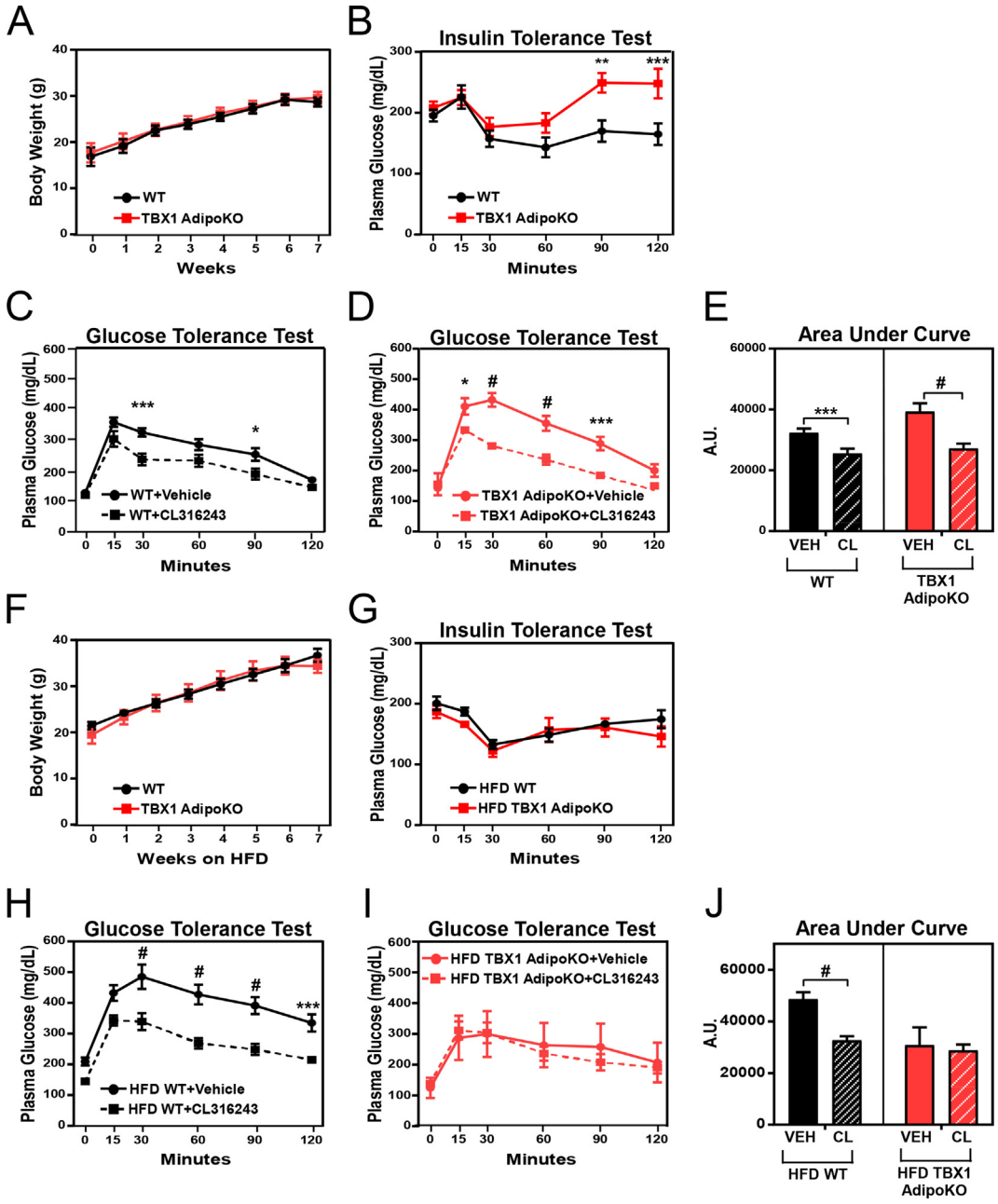


**Figure 2: Adipose TBX1 is required for glucose homeostasis and β-adrenergic responsiveness *in vivo*.** (A) Body weight of chow fed wild type (WT) and TBX1 AdipoKO mice (n = 5–9/group). (B) Plasma glucose levels of chow fed wild type and TBX1 AdipoKO mice during ITT (n = 6/group). Glucose homeostasis was assessed in response to $\beta_3$-adrenergic activation. (C) Plasma glucose levels during a GTT for chow fed wild type mice treated with vehicle or CL316,243 once daily for 3 days prior to GTT (n = 5–9/group). (D) Plasma glucose levels during a GTT for chow fed TBX1 AdipoKO mice treated with vehicle or CL316,243 once daily for 3 days prior to GTT (n = 5–9/group). (E) Area under the curve for plasma glucose levels presented in (C–D). (F) Body weight of wild type and TBX1 AdipoKO mice on high fat diet for 7 weeks (n = 7–12/group) and (G) plasma glucose levels during an ITT of wild type and TBX1 AdipoKO mice on a high fat diet (n = 6/group). (H) Plasma glucose levels during a GTT of high fat diet wild type mice treated with vehicle or CL316,243 once daily for 3 days prior to GTT (n = 5/group). (I) Plasma glucose levels during a GTT for TBX1 AdipoKO mice on high fat diet treated with vehicle or CL316,243 once daily for 3 days prior to GTT (n = 5/group). (J) Area under the curve for plasma glucose levels presented in (H–I). Values are mean ± SEM. *, $p \leq 0.05$; **, $p \leq 0.001$; ***, $p \leq 0.005$; #, $p \leq 0.001$.

derived mesenchymal stem cells were indeed bona fide stem cells as they stained positive and negative for MSC specific surface markers including CD 105, CD 90, and CD 73 (Supplementary Figure. 3C); criteria established by the International Society for Cellular Therapy [37]. To validate these stem cells as a model for testing the function of TBX1 in human adipogenesis, we assessed the adipogenic potential of the human adipose mesenchymal stem cells by performing a standard differentiation protocol (please see Methods) and then quantified adipogenic gene expression and lipid accumulation. Following just 7 days of incubation in a standard differentiation cocktail, key adipogenic genes, including master regulators *CEBPA* and *PPARG*, were significantly increased relative

 

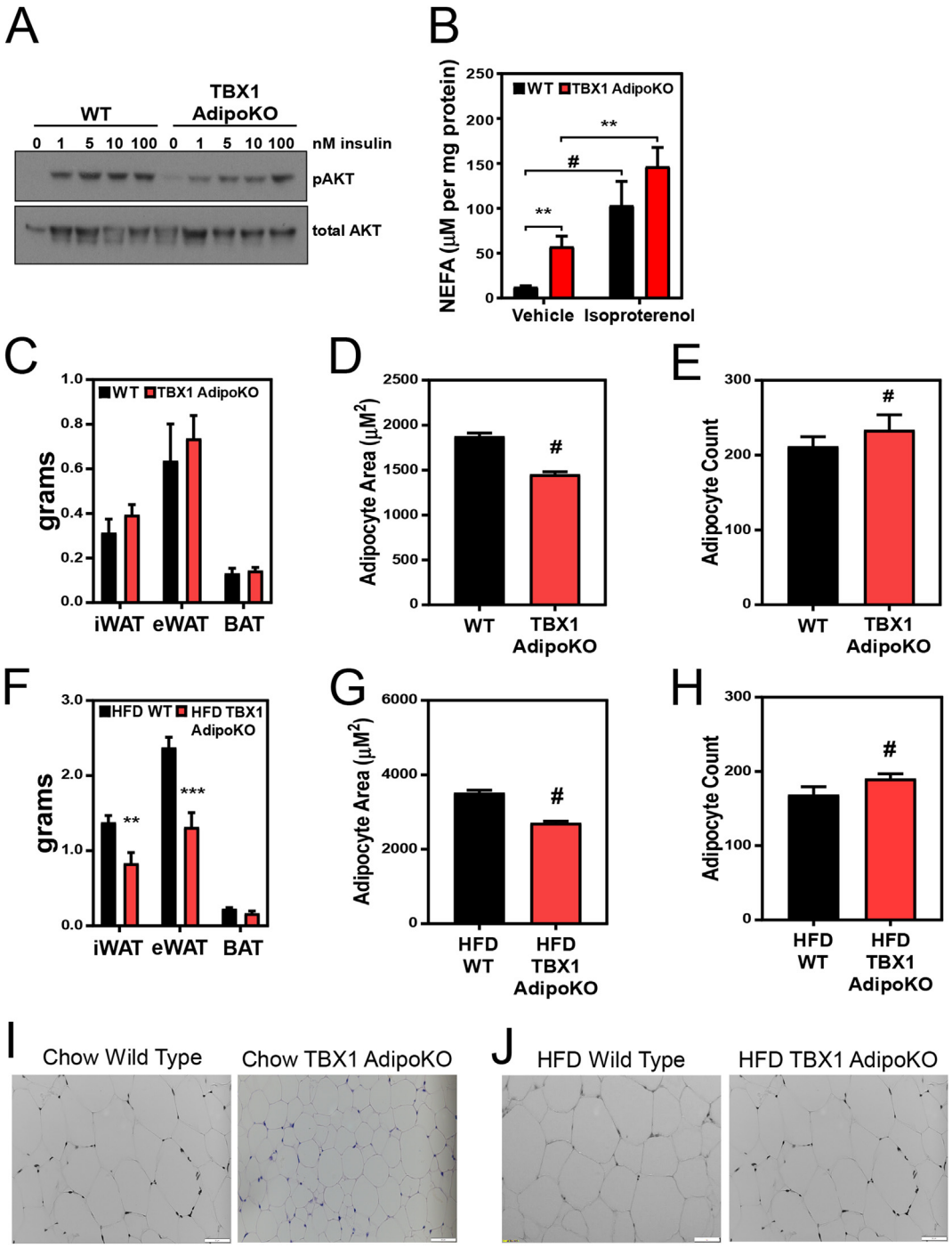


**Figure 3: Insulin and β-adrenergic signaling are altered in subcutaneous adipose tissue of TBX1 AdipoKO mice**. (A) Levels of Akt phosphorylation in response to insulin treatment in iWAT of lean WT and TBX1 AdipoKO mice cultured ex vivo (n = 5 pooled/group). (B) Levels of non-esterified fatty acids released from WT and TBX1 AdipoKO iWAT explants in response to vehicle or isoproterenol treatment (n = 3/group). (C–E) Adipose depot mass (n = 5–9/group) and adipocyte area and count from the iWAT of chow fed wild type and TBX1 AdipoKO mice (n = 3/group). (F–H) Adipose depot mass (n = 5/group) and adipocyte area and count from the iWAT of wild type and TBX1 AdipoKO mice on high fat diet (n = 3/group). Representative H&E images from iWAT of chow fed, 12-week-old wild type and TBX1 AdipoKO mice (I), and wild type and TBX1 AdipoKO mice fed high fat diet for 7 weeks (J). Values are mean ± SEM; *, $p \leq 0.05$; **, $p \leq 0.01$; ***, $p \leq 0.005$; #, $p \leq 0.001$.

to untreated cells (Figure 3C) and lipid accumulation was visible in cells treated with the differentiation cocktail and stained with AdipoRed (Supplementary Figure. 3D). Additionally, *TBX1* mRNA was significantly increased in human adipose mesenchymal stem cells on the seventh day of treatment with the differentiation cocktail (Figure 4D), linking increased TBX1 expression in human mesenchymal stem cells with the adipogenic program. To directly test this, we again used a siRNA mediated approach to evaluate the requirement of TBX1 expression during adipogenesis in human cells. As seen in Figure 4E,A greater than 50% reduction in

 

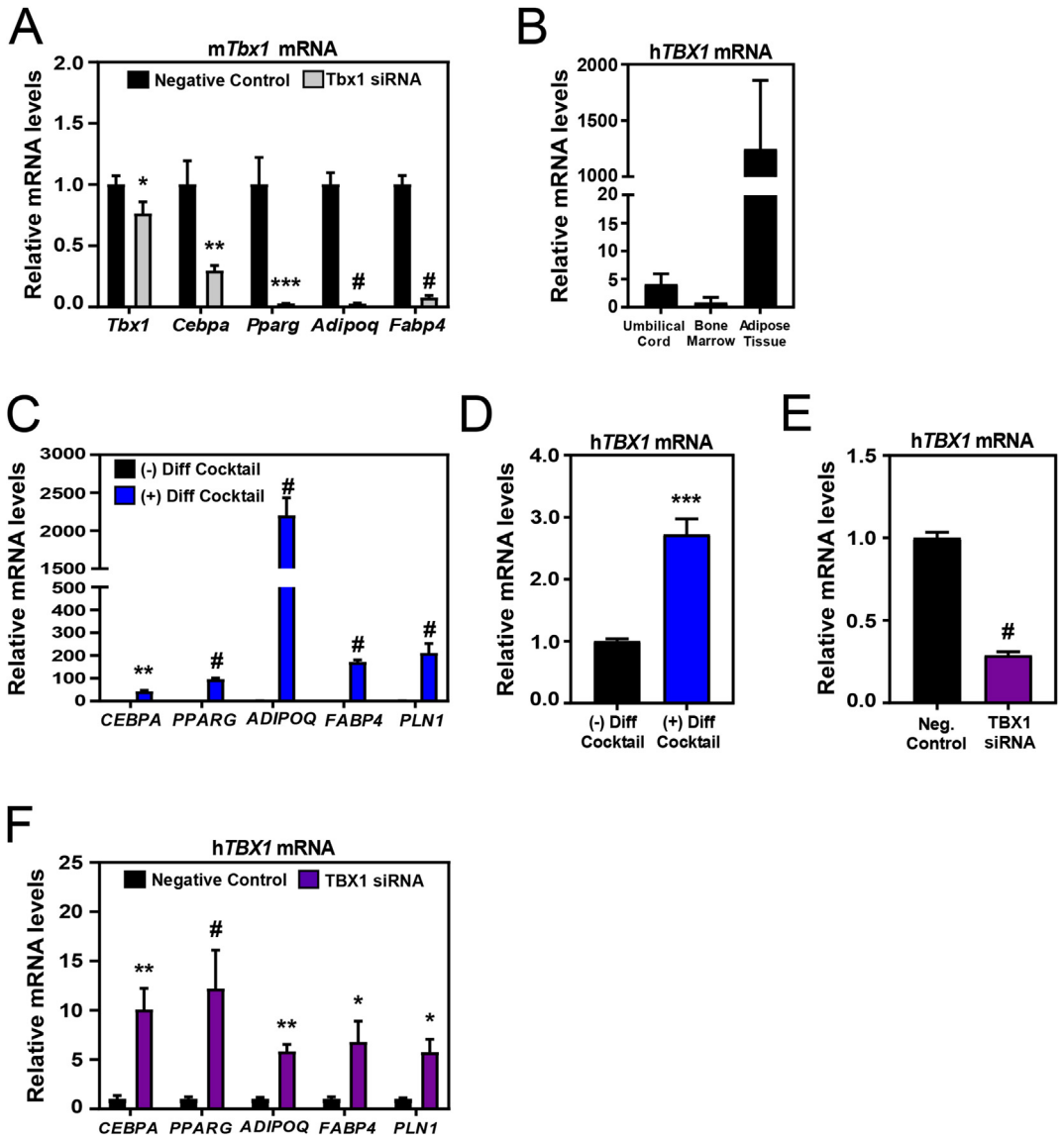


**Figure 4: TBX1 differentially regulates murine versus human adipogenesis**. (A) Adipocyte gene expression in mouse adipose derived stromal vascular cells transfected with a negative control scrambled siRNA or *Tbx1* siRNA and then treated with differentiation cocktail containing 1 μM dexamethasone, 0.5 mM IBMX and 5 μg/mL insulin for 48 h (n = 3 independent experiments). (B) *TBX1* mRNA in stem cells isolated from various human tissue sources (multiple donors). (C) *TBX1* mRNA from undifferentiated ((−) Diff Cocktail) versus differentiated ((+) Diff Cocktail) human adipose mesenchymal stem cells (n = 3 independent experiments). Differentiation cocktail containing 1 μM dexamethasone, 0.5 mM IBMX and 5 μg/mL insulin for 7 days. (D) *TBX1* mRNA in human adipose mesenchymal stem cells treated without differentiation cocktail ((−) Diff Cocktail) or with differentiation cocktail ((+) Diff Cocktail) for 7 days (n = 3 independent experiments). (E) *TBX1* mRNA in human adipose mesenchymal stem cells transfected with either a negative control scrambled siRNA or TBX1 siRNA and then differentiated as described above (n = 3 independent experiments). (F) Adipocyte gene expression in human adipose mesenchymal stem cells transfected with a negative control scrambled siRNA or *TBX1* siRNA and then treated with differentiation cocktail (n = 3 independent experiments). Values are mean ± SEM.

*TBX1* mRNA was observed in TBX1 siRNA transfected human adipose mesenchymal stem cells differentiated for 7 days with near maximal transfection efficiency (Supplementary Figure. 3E). Furthermore, the decreased *TBX1* expression due siRNA transduction resulted in significantly increased expression of adipogenic genes (Figure 4F). These results indicate that proper expression of TBX1 in both murine and human adipose stem cells is essential for proper adipogenesis, albeit in a divergent, species-specific manner.

## 4. DISCUSSION

The activation of UCP1$^{+}$ adipose tissue enhances adaptive thermogenesis resulting in the clearance of significant levels of glucose and lipid from circulation [7]. In rodents, adipose 'beiging' can prevent the development of diet-induced obesity and dramatically improve metabolic parameters, suggesting that activation of beige adipose could serve as a therapeutic approach to combat human obesity [10–12]. In mice, the subcutaneous inguinal white adipose depot is particularly

 

susceptible to beiging [6], and a number of developmental genes including *HOX* family genes, *Shox2*, and *Tbx15* are preferentially expressed in the subcutaneous adipose depot of both rodents and humans [49—53]. TBX1 has also served as a genetic marker of beige adipose in vivo for both rodents and humans [14,20—22], yet its function in adipose tissue has not been previously reported. Consistent with previous studies, we found TBX1 to be highly expressed in the subcutaneous adipose of mice. Thus we generated mice genetically overexpressing or lacking TBX1 expression specifically in adipose tissues (TBX1 AdipoTG and TBX1 AdipoKO mice, respectively) in order to directly test the function of TBX1 in this tissue. Overexpression of TBX1 in adipose tissues is not sufficient to fully drive the beiging of white adipose tissue as TBX1 AdipoTG mice did not display differences in beige cell number in subcutaneous inguinal white adipose tissue and were not protected against cold induced decreases in body temperature or diet induced obesity. Importantly, we did not observe increases in any other genetic markers of beige adipose tissue or mitochondrial biogenesis (Supplementary Figures. 2G—J) [41], suggesting that TBX1 may regulate adipose UCP1 expression, but that transgenic overexpression of TBX1 is not sufficient to 'trans-differentiate' mature, adiponectin expressing white adipose into metabolically active beige adipose tissue.

Although our data indicates that TBX1 is not sufficient to convert mature adipose into thermogenic beige adipose, its expression in adipose tissue and resident beige cells is required for the defense of body temperature during cold and to maintain β-adrenergic responsiveness and glucose homeostasis in vivo. TBX1 AdipoKO mice housed in the cold for 3 days displayed a significant decrease in body temperature compared to control mice (Figure 1M). Complementary in vitro and ex vivo studies using TBX1 AdipoKO adipocytes and isolated mitochondria support the notion that TBX1 functions in a cell autonomous manner to regulate UCP1 expression and activity rather than regulating beige adipocyte formation. In this regard, TBX1 could regulate adipocyte UCP1 expression via two primary potential mechanisms: 1) direct transcriptional regulation via binding to regulatory sequences in the *Ucp1* gene, and/or 2) by altering β-adrenergic signaling dynamics within adipose tissue. Notably, ChIP-seq analysis using mouse embryonic cardiac cells identified a region within the *Ucp1* gene enriched for a TBX1 binding motif [27]. This direct DNA-binding mechanism of action would be similar to that recently reported for another T-box 1 family member, TBX15. Using adipose-specific TBX15 knockout mice and ChIP analysis, Sun et al. demonstrated that TBX15 is required for adrenergically activated adipose beiging by binding to a region within the *Prdm16* promoter [54]. In contrast to the effects of TBX15, our in vivo and in vitro data suggest that TBX1 primarily regulates β-adrenergic versus insulin signaling within adipose tissue as well as β-adrenergic responsiveness in vivo. Loss of adipose TBX1 expression resulted in elevated fasting plasma glucose levels as well as increased plasma glucose levels during the later time points of an ITT (Figure 2B; time 90 and 120 min). Plasma glucose levels at these latter time points reflect the actions of counterregulatory mechanisms, such as catecholamines and cortisol, that occur in response to the insulin induced hypoglycemia that occurs earlier during the ITT [44,45]. Thus our data indicate that although TBX1 AdipoKO mice and littermate controls have comparable insulin sensitivity, TBX1 AdipoKO mice have a potentially enhanced counterregulatory response compared to control mice following the initial clearance of plasma glucose in response to insulin.

In chow fed TBX1 AdipoKO mice, TBX1 expression was dispensable for $\beta_3$-adrenergic mediated glucose clearance. Conversely, in high fat diet TBX1 AdipoKO mice adipose TBX1 expression was required for $\beta_3$-adrenergic mediated glucose clearance. CL316,243 induces beige adipocytes in a manner similar to yet independent of cold exposure [36] and stimulates glucose uptake in vivo [55]. In our GTT studies, TBX1 AdipoKO mice were injected once daily for 3 days with CL315,243. On the third day, 6 h following the final CL316,243 injection, a GTT was performed in order to directly test the loss of adipose TBX1 on $\beta_3$-adrenergic regulated glucose homeostasis. Notably, CL316,243 treatment acutely ($<$2 h) stimulates free fatty acid induced insulin secretion [56]. However, plasma levels of CL316,243 are significantly reduced 6-hours post-injection which is in line with the timing of our GTT studies [57]. Since whole-body insulin sensitivity and plasma non-esterified fatty acid levels between high fat diet TBX1 AdipoKO and wild type mice were comparable, our findings support that the loss of TBX1 from adipose tissue during a high fat feeding affects β-adrenergic mediated glucose disposal [58]. That is, if basal β-adrenergic responsiveness is already enhanced, further glucose clearing by $\beta_3$-adrenergic stimulation may not be observed [58]. Thus TBX1 may regulate β-adrenergic responsiveness of adipose tissue and mediate crosstalk between β-adrenergic and insulin signaling within adipose, not unlike what has been reported in the heart [59,60]. This notion is supported by the impaired insulin signaling and enhanced basal lipolysis rates using the iWAT from TBX1 AdipoKO mice. In line with the notion that TBX1 regulates the β-adrenergic responsiveness of subcutaneous adipose, overexpression of the TBX1 family member TBX15 in 3T3-L1 adipocytes was sufficient to increase basal lipolysis and decrease mitochondrial respiration [61] while the genetic deletion of the developmental gene *Shox2*, specifically in adipose tissue, resulted in smaller subcutaneous adipocytes and loss of subcutaneous adipose due to enhanced lipolysis in vivo [62]. Similar to the phenotype of the adipose-specific *Shox2* knockout mice, the hypomorphic iWAT adipocytes observed in our TBX1 AdipoKO mice are likely a result of the impaired insulin signaling and concomitant increased rate of lipolysis. Overall, these studies using TBX1 AdipoKO iWAT ex vivo directly link metabolic dysfunction and altered insulin signaling in this adipose depot with the altered β-adrenergic responsiveness of TBX1 AdipoKO mice observed in vivo.

The metabolic phenotype of our TBX1 AdipoKO mice are both similar and divergent from a recent report characterizing adipose specific TBX15 knockout mice [54]. Similar to our findings, the TBX15 adipose knockout mice lacked expression of UCP1 in the subcutaneous inguinal white adipose depot following cold exposure and treatment with the $\beta_3$-adrenergic agonist CL316,243 [54]. However, TBX15 adipose knockout mice displayed basal insulin resistance and gained more weight on a high fat diet concomitant to decreased energy expenditure [54], which was not observed in our TBX1 AdipoKO mice. The more pronounced metabolic phenotype of the TBX15 adipose knockout mice is likely attributed to the transcriptional effects of TBX15 via direct DNA binding in the *Prdm16* promoter region [54]. Although TBX1 shares a conserved DNA binding T-box domain as TBX15, data from the literature supports the hypothesis that TBX1 exerts its effects not through direct DNA binding but rather via off-DNA binding through protein-protein interactions including SMAD family proteins and components of the chromatin remodeling complex as well as histone methyl-transferases [27—29].

While our primary focus was to test the function of TBX1 in mature adipose tissue, we also discovered that TBX1 expression is enriched in

 

mouse stromal vascular cells and human adipose derived mesenchymal stem cells. Although several developmental genes are differentially expressed in various adipose depots of rodents and humans [51,52,63], no reports exist concerning TBX1 function in human adipose tissue. Since TBX1 is important for the development of a variety of cell types [24], we tested its function during adipogenesis of both murine and human derived stem cells via a siRNA mediated approach. Surprisingly, TBX1 knockdown via siRNA had differential effects upon adipogenesis in murine versus human derived stem cells. While reduced *Tbx1* expression in mouse cells significantly reduced adipocyte gene expression post-differentiation, a significant reduction in *TBX1* expression in human stem cells significantly enhanced adipocyte gene expression post-differentiation. The impairment in the differentiation of mouse derived stromal vascular cells into adipocytes is similar to what was reported with the stable overexpression of TBX15 in mouse derived 3T3-L1 cells [61], suggesting that TBX1 and TBX15 may function through transcriptionally distinct mechanisms in order to exert similar outcomes upon murine adipocyte differentiation. The process of adipocyte differentiation is complex and involves coordinated protein-DNA and protein-protein interactions. Overall, the process involves the commitment of mesenchymal stem cells into a pre-adipocyte lineage followed by adipocyte specific gene expression and lipid accumulation as the pre-adipocyte differentiates into a fully mature adipocyte [64]. Notably, the cellular conversion from mesenchymal stem cell into pre-adipocyte involves the coordinated action of several developmental genes including WNT, BMP, TGFβ and SMAD family member proteins [64]; each of which TBX1 has been reported to interact with [28,29,46,65]. Therefore it is plausible that TBX1 interacts with these proteins in a species-specific manner to modulate adipocyte differentiation. Furthermore, TBX1 has been reported to regulate stem cells in the developing heart, the hair follicle niche, and in smooth muscle [46–48] and to interact with the chromatin remodeling complex [29] as well as histone methyltransferases in order to regulate chromatin structure during the differentiation of cardiac cells [27]. Therefore it is plausible that TBX1 may differentially interact with any combination of key components in order to exert opposite effects on adipogenesis in mouse versus human cells. Finally, mouse adipose stromal vascular cells and human adipose derived mesenchymal stem cell populations are composed of a heterogenous cell populations [66], and although there is overlap between species, the specific cell type(s) expressing TBX1 in human versus mouse cells could potentially underlie the observed differential species-specific effects upon adipogenesis.

In summary, overexpression of adipose TBX1 increased UCP1 expression in vivo; however, this induction of UCP1 was not sufficient to drive a beiging phenotype in vivo. Thus solely targeting adipose TBX1 expression is likely not an optimal therapeutic target for increasing adipose beiging as an approach for treating obesity. However, adipose TBX1 is required in vivo for the regulation of body temperature and UCP1 expression in response to β-adrenergic stimulation, adipose insulin signaling and overall $\beta_3$-adrenergic mediated glucose homeostasis in vivo. Additionally, TBX1 expression is required for the differentiation of mouse stromal vascular cells but its decreased expression enhances the differentiation of human mesenchymal stem cells into adipocytes indicating a significant yet species-specific role for TBX1 in adipocyte differentiation. This effect in human mesenchymal stem cells warrants further investigation as dysfunctional mesenchymal stem cells during obesity contribute significantly to overall adipose dysfunction [67]. These studies identify adipose TBX1 as a novel regulator of energy homeostasis, metabolic signaling and adipocyte growth, development and differentiation, but exactly how TBX1 regulates metabolic signaling specifically in subcutaneous adipose tissue, whether through direct DNA binding and/or through off-DNA protein-protein interactions, warrants future investigation.

## ACKNOWLEDGEMENTS

The authors thank Drs. Adam Rauckhorst and Brett Wagner (University of Iowa) for technical assistance and insightful discussions. This work was supported by the National Institutes of Health (NIH) K01DK111758 (K R M), R01DK106104 (M.J.P.), F32 DK117510 (K.E.C.), and in part by the National Cancer Institute, NIH) P30CA086862 (University of Iowa ESR Core). K.R.M. conceived of, designed and conducted experiments. L.K.B., A.Q.K.M., K.E.C, M.P.L., M.K.K. and M.M.S. conducted experiments and performed data analysis. K.R.M. and M.J.P. wrote the manuscript. K.R.M is the guarantor of this work and, as such, had full access to all the data in the study and takes responsibility for the integrity of the data and the accuracy of the data analysis.

## CONFLICT OF INTEREST

None declared.

## APPENDIX A. SUPPLEMENTARY DATA

Supplementary data to this article can be found online at https://doi.org/10.1016/j.molmet.2020.02.008.

## REFERENCES

[1] Lynes, M.D., Tseng, Y.H., 2018. Deciphering adipose tissue heterogeneity. Annals of the New York Academy of Sciences 1411(1):5–20.
[2] Kusminski, C.M., Bickel, P.E., Scherer, P.E., 2016. Targeting adipose tissue in the treatment of obesity-associated diabetes. Nature Reviews Drug Discovery 15(9):639–660.
[3] Collaborators, G.B.D.O., Afshin, A., Forouzanfar, M.H., Reitsma, M.B., Sur, P., Estep, K., et al., 2017. Health effects of overweight and obesity in 195 countries over 25 years. New England Journal of Medicine 377(1): 13–27.
[4] Cannon, B., Nedergaard, J., 2004. Brown adipose tissue: function and physiological significance. Physiological Reviews 84(1):277–359.
[5] Inagaki, T., Sakai, J., Kajimura, S., 2016. Transcriptional and epigenetic control of brown and beige adipose cell fate and function. Nature Reviews Molecular Cell Biology 17(8):480–495.
[6] Seale, P., Kajimura, S., Yang, W., Chin, S., Rohas, L.M., Uldry, M., et al., 2007. Transcriptional control of brown fat determination by PRDM16. Cell Metabolism 6(1):38–54.
[7] Bartelt, A., Bruns, O.T., Reimer, R., Hohenberg, H., Ittrich, H., Peldschus, K., et al., 2011. Brown adipose tissue activity controls triglyceride clearance. Nature Medicine 17(2):200–205.
[8] Bi, P., Shan, T., Liu, W., Yue, F., Yang, X., Liang, X.R., et al., 2014. Inhibition of Notch signaling promotes browning of white adipose tissue and ameliorates obesity. Nature Medicine 20(8):911–918.
[9] Wang, H., Liu, L., Lin, J.Z., Aprahamian, T.R., Farmer, S.R., 2016. Browning of white adipose tissue with roscovitine induces a distinct population of UCP1(+) adipocytes. Cell Metabolism 24(6):835–847.
[10] Kajimura, S., Spiegelman, B.M., Seale, P., 2015. Brown and beige fat: physiological roles beyond heat generation. Cell Metabolism 22(4):546–559.

 

[11] Kim, S.H., Plutzky, J., 2016. Brown fat and browning for the treatment of obesity and related metabolic disorders. Diabetes & Metabolism J 40(1): 12–21.
[12] Harms, M., Seale, P., 2013. Brown and beige fat: development, function and therapeutic potential. Nature Medicine 19(10):1252–1263.
[13] Wang, Q.A., Tao, C., Gupta, R.K., Scherer, P.E., 2013. Tracking adipogenesis during white adipose tissue development, expansion and regeneration. Nature Medicine 19(10):1338–1344.
[14] Rosenwald, M., Perdikari, A., Rulicke, T., Wolfrum, C., 2013. Bi-directional interconversion of brite and white adipocytes. Nature Cell Biology 15(6):659–667.
[15] Barbatelli, G., Murano, I., Madsen, L., Hao, Q., Jimenez, M., Kristiansen, K., et al., 2010. The emergence of cold-induced brown adipocytes in mouse white fat depots is determined predominantly by white to brown adipocyte transdifferentiation. American Journal of Physiology. Endocrinology and Metabolism 298(6):E1244–E1253.
[16] Himms-Hagen, J., Melnyk, A., Zingaretti, M.C., Ceresi, E., Barbatelli, G., Cinti, S., 2000. Multilocular fat cells in WAT of CL-316243-treated rats derive directly from white adipocytes. American Journal of Physiology - Cell Physiology 279(3):C670–C681.
[17] Vitali, A., Murano, I., Zingaretti, M.C., Frontini, A., Ricquier, D., Cinti, S., 2012. The adipose organ of obesity-prone C57BL/6J mice is composed of mixed white and brown adipocytes. The Journal of Lipid Research 53(4): 619–629.
[18] Ussar, S., Lee, K.Y., Dankel, S.N., Boucher, J., Haering, M.F., Kleinridders, A., et al., 2014. ASC-1, PAT2, and P2RX5 are cell surface markers for white, beige, and brown adipocytes. Science Translational Medicine 6(247): 247ra103.
[19] Steinbring, J., Graja, A., Jank, A.M., Schulz, T.J., 2017. Flow cytometric isolation and differentiation of adipogenic progenitor cells into Brown and brite/beige adipocytes. Methods in Molecular Biology 1566:25–36.
[20] de Jong, J.M., Larsson, O., Cannon, B., Nedergaard, J., 2015. A stringent validation of mouse adipose tissue identity markers. American Journal of Physiology. Endocrinology and Metabolism 308(12):E1085–E1105.
[21] Wu, J., Bostrom, P., Sparks, L.M., Ye, L., Choi, J.H., Giang, A.H., et al., 2012. Beige adipocytes are a distinct type of thermogenic fat cell in mouse and human. Cell 150(2):366–376.
[22] Jespersen, N.Z., Larsen, T.J., Peijs, L., Daugaard, S., Homoe, P., Loft, A., et al., 2013. A classical brown adipose tissue mRNA signature partly overlaps with brite in the supraclavicular region of adult humans. Cell Metabolism 17(5): 798–805.
[23] Papaioannou, V.E., 2014. The T-box gene family: emerging roles in development, stem cells and cancer. Development 141(20):3819–3833.
[24] Baldini, A., Fulcoli, F.G., Illingworth, E., 2017. Tbx1: transcriptional and developmental functions. Current Topics in Developmental Biology 122:223–243.
[25] McDonald-McGinn, D.M., Sullivan, K.E., Marino, B., Philip, N., Swillen, A., Vorstman, J.A., et al., 2015. 22q11.2 deletion syndrome. Nature Reviews Disease Primers 1:15071.
[26] Castellanos, R., Xie, Q., Zheng, D., Cvekl, A., Morrow, B.E., 2014. Mammalian TBX1 preferentially binds and regulates downstream targets via a tandem T-site repeat. PloS One 9(5):e95151.
[27] Fulcoli, F.G., Franzese, M., Liu, X., Zhang, Z., Angelini, C., Baldini, A., 2016. Rebalancing gene haploinsufficiency in vivo by targeting chromatin. Nature Communications 7:11688.
[28] Fulcoli, F.G., Huynh, T., Scambler, P.J., Baldini, A., 2009. Tbx1 regulates the BMP-Smad1 pathway in a transcription independent manner. PloS One 4(6): e6049.
[29] Chen, L., Fulcoli, F.G., Ferrentino, R., Martucciello, S., Illingworth, E.A., Baldini, A., 2012. Transcriptional control in cardiac progenitors: Tbx1 interacts with the BAF chromatin remodeling complex and regulates Wnt5a. PLoS Genetics 8(3):e1002571.
[30] Eguchi, J., Wang, X., Yu, S., Kershaw, E.E., Chiu, P.C., Dushay, J., et al., 2011. Transcriptional control of adipose lipid handling by IRF4. Cell Metabolism 13(3):249–259.
[31] Vitelli, F., Huynh, T., Baldini, A., 2009. Gain of function of Tbx1 affects pharyngeal and heart development in the mouse. Genesis 47(3):188–195.
[32] Xu, H., Morishima, M., Wylie, J.N., Schwartz, R.J., Bruneau, B.G., Lindsay, E.A., et al., 2004. Tbx1 has a dual role in the morphogenesis of the cardiac outflow tract. Development 131(13):3217–3227.
[33] Markan, K.R., Naber, M.C., Ameka, M.K., Anderegg, M.D., Mangelsdorf, D.J., Kliewer, S.A., et al., 2014. Circulating FGF21 is liver derived and enhances glucose uptake during refeeding and overfeeding. Diabetes 63(12):4057–4063.
[34] Markan, K.R., Naber, M.C., Small, S.M., Peltekian, L., Kessler, R.L., Potthoff, M.J., 2017. FGF21 resistance is not mediated by downregulation of beta-klotho expression in white adipose tissue. Molecular Metabolism 6(6): 602–610.
[35] Gray, L.R., Rauckhorst, A.J., Taylor, E.B., 2016. A method for multiplexed measurement of mitochondrial pyruvate carrier activity. Journal of Biological Chemistry 291(14):7409–7417.
[36] Shao, M., Ishibashi, J., Kusminski, C.M., Wang, Q.A., Hepler, C., Vishvanath, L., et al., 2016. Zfp423 maintains white adipocyte identity through suppression of the beige cell thermogenic gene program. Cell Metabolism 23(6):1167–1184.
[37] Dominici, M., Le Blanc, K., Mueller, I., Slaper-Cortenbach, I., Marini, F., Krause, D., et al., 2006. Minimal criteria for defining multipotent mesenchymal stromal cells. The International Society for Cellular Therapy position statement. Cytotherapy 8(4):315–317.
[38] Boland, L., Burand, A.J., Brown, A.J., Boyt, D., Lira, V.A., Ankrum, J.A., 2018. IFN-gamma and TNF-alpha pre-licensing protects mesenchymal stromal cells from the pro-inflammatory effects of palmitate. Molecular Therapy 26(3):860–873.
[39] Boland, L.K., Burand, A.J., Boyt, D.T., Dobroski, H., Di, L., Liszewski, J.N., et al., 2019. Nature vs. Nurture: defining the effects of mesenchymal stromal cell isolation and culture conditions on resiliency to palmitate challenge. Frontiers in Immunology 10:1080.
[40] Klingelhutz, A.J., Gourronc, F.A., Chaly, A., Wadkins, D.A., Burand, A.J., Markan, K.R., et al., 2018. Scaffold-free generation of uniform adipose spheroids for metabolism research and drug discovery. Scientific Reports 8(1): 523.
[41] Fisher, F.M., Kleiner, S., Douris, N., Fox, E.C., Mepani, R.J., Verdeguer, F., et al., 2012. FGF21 regulates PGC-1alpha and browning of white adipose tissues in adaptive thermogenesis. Genes & Development 26(3):271–281.
[42] Seale, P., Conroe, H.M., Estall, J., Kajimura, S., Frontini, A., Ishibashi, J., et al., 2011. Prdm16 determines the thermogenic program of subcutaneous white adipose tissue in mice. Journal of Clinical Investigation 121(1):96–105.
[43] Cannon, B., Nedergaard, J., 2011. Nonshivering thermogenesis and its adequate measurement in metabolic studies. Journal of Experimental Biology 214(Pt 2):242–253.
[44] Ayala, J.E., Samuel, V.T., Morton, G.J., Obici, S., Croniger, C.M., Shulman, G.I., et al., 2010. Standard operating procedures for describing and performing metabolic tests of glucose homeostasis in mice. Disease Model Mechanism 3(9–10):525–534.
[45] Alquier, T., Poitout, V., 2018. Considerations and guidelines for mouse metabolic phenotyping in diabetes research. Diabetologia 61(3):526–538.

 

[46] Chen, T., Heller, E., Beronja, S., Oshimori, N., Stokes, N., Fuchs, E., 2012. An RNA interference screen uncovers a new molecule in stem cell self-renewal and long-term regeneration. Nature 485(7396):104–108.

[47] Yan, Y., Su, M., Song, Y., Tang, Y., Tian, X.C., Rood, D., et al., 2014. Tbx1 modulates endodermal and mesodermal differentiation from mouse induced pluripotent stem cells. Stem Cells and Development 23(13):1491–1500.

[48] Hirschi, K.K., Majesky, M.W., 2004. Smooth muscle stem cells. Anatomical Record, The, Part A: Discoveries in Molecular, Cellular, and Evolutionary Biology 276(1):22–33.

[49] Vohl, M.C., Sladek, R., Robitaille, J., Gurd, S., Marceau, P., Richard, D., et al., 2004. A survey of genes differentially expressed in subcutaneous and visceral adipose tissue in men. Obesity Research 12(8):1217–1222.

[50] Cantile, M., Procino, A., D'Armiento, M., Cindolo, L., Cillo, C., 2003. HOX gene network is involved in the transcriptional regulation of in vivo human adipogenesis. Journal of Cellular Physiology 194(2):225–236.

[51] Gesta, S., Bluher, M., Yamamoto, Y., Norris, A.W., Berndt, J., Kralisch, S., et al., 2006. Evidence for a role of developmental genes in the origin of obesity and body fat distribution. Proceedings of the National Academy of Sciences of the United States of America 103(17):6676–6681.

[52] Yamamoto, Y., Gesta, S., Lee, K.Y., Tran, T.T., Saadatirad, P., Kahn, C.R., 2010. Adipose depots possess unique developmental gene signatures. Obesity 18(5):872–878.

[53] Tchkonia, T., Lenburg, M., Thomou, T., Giorgadze, N., Frampton, G., Pirtskhalava, T., et al., 2007. Identification of depot-specific human fat cell progenitors through distinct expression profiles and developmental gene patterns. American Journal of Physiology. Endocrinology and Metabolism 292(1):E298–E307.

[54] Sun, W., Zhao, X., Wang, Z., Chu, Y., Mao, L., Lin, S., et al., 2019. Tbx15 is required for adipocyte browning induced by adrenergic signaling pathway. Molecular Metabolism.

[55] de Souza, C.J., Hirshman, M.F., Horton, E.S., 1997. CL-316,243, a beta3-specific adrenoceptor agonist, enhances insulin-stimulated glucose disposal in nonobese rats. Diabetes 46(8):1257–1263.

[56] MacPherson, R.E., Castellani, L., Beaudoin, M.S., Wright, D.C., 2014. Evidence for fatty acids mediating CL 316,243-induced reductions in blood glucose in mice. American Journal of Physiology. Endocrinology and Metabolism 307(7):E563–E570.

[57] Danysz, W., Han, Y., Li, F., Nicoll, J., Buch, P., Hengl, T., et al., 2018. Browning of white adipose tissue induced by the ss3 agonist CL-316,243 after local and systemic treatment - PK-PD relationship. Biochimica et Biophysica Acta - Molecular Basis of Disease 1864(9 Pt B):2972–2982.

[58] Mukaida, S., Evans, B.A., Bengtsson, T., Hutchinson, D.S., Sato, M., 2017. Adrenoceptors promote glucose uptake into adipocytes and muscle by an insulin-independent signaling pathway involving mechanistic target of rapamycin complex 2. Pharmacological Research 116:87–92.

[59] Fu, Q., Xu, B., Parikh, D., Cervantes, D., Xiang, Y.K., 2015. Insulin induces IRS2-dependent and GRK2-mediated beta2AR internalization to attenuate betaAR signaling in cardiomyocytes. Cellular Signalling 27(3):707–715.

[60] Ciccarelli, M., Chuprun, J.K., Rengo, G., Gao, E., Wei, Z., Peroutka, R.J., et al., 2011. G protein-coupled receptor kinase 2 activity impairs cardiac glucose uptake and promotes insulin resistance after myocardial ischemia. Circulation 123(18):1953–1962.

[61] Gesta, S., Bezy, O., Mori, M.A., Macotela, Y., Lee, K.Y., Kahn, C.R., 2011. Mesodermal developmental gene Tbx15 impairs adipocyte differentiation and mitochondrial respiration. Proceedings of the National Academy of Sciences of the United States of America 108(7):2771–2776.

[62] Lee, K.Y., Yamamoto, Y., Boucher, J., Winnay, J.N., Gesta, S., Cobb, J., et al., 2013. Shox2 is a molecular determinant of depot-specific adipocyte function. Proceedings of the National Academy of Sciences of the United States of America 110(28):11409–11414.

[63] Lee, K.Y., Sharma, R., Gase, G., Ussar, S., Li, Y., Welch, L., et al., 2017. Tbx15 defines a glycolytic subpopulation and white adipocyte heterogeneity. Diabetes 66(11):2822–2829.

[64] Cristancho, A.G., Lazar, M.A., 2011. Forming functional fat: a growing understanding of adipocyte differentiation. Nature Reviews Molecular Cell Biology 12(11):722–734.

[65] Huh, S.H., Ornitz, D.M., 2010. Beta-catenin deficiency causes DiGeorge syndrome-like phenotypes through regulation of Tbx1. Development 137(7):1137–1147.

[66] Merrick, D., Sakers, A., Irgebay, Z., Okada, C., Calvert, C., Morley, M.P., et al., 2019. *Identification of a mesenchymal progenitor cell hierarchy in adipose tissue*. Science 364(6438).

[67] Louwen, F., Ritter, A., Kreis, N.N., Yuan, J., 2018. Insight into the development of obesity: functional alterations of adipose-derived mesenchymal stem cells. Obesity Reviews 19(7):888–904.

 